3-D Reconstruction for SMT Solder Joint Based on Joint Shadow

Lichen Wang[1], Aimin Zhang[1], Chujia Guo[1], Songyun Zhao[1], Pervez Bhan[1]

1. School of Electronic & Information Engineering, Xi'an Jiaotong University, Xi'an, 710049, China
E-mail: wanglichenxj@gmail.com
E-mail: zhangam@mail.xjtu.edu.cn

Abstract:

3-D reconstruction is essential for Surface Mount Technology (SMT) solder joint defect inspection. Conventional vision-based reconstruction methods are very sensitive to the surface reflectivity variation or require sequential images from multicamera system which would increase calibration difficulty and computation complexity.

To solve the problem mentioned above, a novel shadow based 3-D reconstruction method for solder joint reconstruction is proposed. A paralleled light casts a joint shadow on PCB (Printed Circuit Board), and then the shadow is captured by a camera and used to reconstruct the joint. To make a single shadow obtain the 3-D model totally, a joint shape model is proposed based on consistent joint characteristics which produced by soldering tin surface tension when the tin is still liquid during the manufactory process. Compare the reconstruction results of this method with that of Shape from Shading (SFS) reconstruction method, this method can reduce the hardware cost and algorithm complexity significantly, which at the same time obtains better accuracy and efficiency.

Key Words: 3-D reconstruction, machine vision, shadow, surface mount technology, illumination model.

1 INTRODUCTION

3-D reconstruction is a basic problem in computer vision and has a wide spectrum of applications, such as manufactory quality control, object recognition, city modeling, video games, surveillance and visualization. The most common reconstruction systems are often built around specialized and expensive hardware (e.g., laser scanner). Other methods based on photogrammetry or computer vision, can instead obtain 3-D models of objects with low cost acquisition systems.

Solder joints quality of SMT component is very important for the quality of electronic products. A large number of vision-based solder joints inspection equipments have been used in market, but most of them generally only work in 2-D testing mode [1-4]. Many defects can only be detected by knowing the 3-D shape of the solder joint, so in the latest years, 3-D reconstruction methods for SMT solder joint have been proposed.

High-speed laser scanner [5-8] is a useful method for reconstruction, however the device is very expensive and the scanner is slow. X-ray is used by some methods to reconstruct [9-12], but the methods are sensitive to the components. A method which uses special structured light to scan and detect the surface of solder joint was proposed by Sanderson and Nayar in [13]. However, this method can't reduce the time consuming in the light scan process and the image process is complicated. Some advanced research in the multilevel modified colorized structured light to improve the detection efficiency [14-17]. Omron Corporation used round multicolor LED light to inspect the joint, but this method doesn't provide 3-D reconstruction information.

Horn proposed a method to reconstruction the surface of moon called Shape from Shading (SFS) [18-19]. This method is based on Lambertian surface model or other surface condition assumptions, so the reflectivity variation and nonuniformity would have significant effect on the reconstruction accuracy, especially the specular reflection from solder joint surface. Many efforts have been done to improve the quality of the result [20-26], but there is still not a universal and compatible way to reconstruct solder joints.

Shadow based reconstruction method is another useful method which is already used in some areas [27-31]. Rafik et al, inspired from the well-known Shape from Silhouettes method, proposed a shadow based method [32] to reconstruct the given object by shadows. Austin Abrams et al proposed a shadow tracking system [33] which tracks thousands of shadows in outdoor images to create a 3-D outdoor scene. Daniel et al [34] and Daum et al [35] introduced methods which used moving shadows to reconstruct. However, these shadow based methods mentioned above need several cameras or several sequential images to reconstruct. The multicamera system can be affected by calibration errors deeply and the system may be expensive. Sequential images would increase the computation complexity significantly. Furthermore, the SMT component size is very small and the height is very low, so the shadow can only be casted in some specific directions. The conventional shadow based methods may not be able to reconstruct when some shadows are missing.

A novel 3-D reconstruction method for SMT solder joint based on a single still shadow image is proposed in this paper. A structured light is used to cast a shadow of joint on the PCB, then a single camera captures an image of the joint

This work is supported by National Nature Science Foundation under Grant (51177126, 61105126).

shadow, finally the shadow is extracted and used to reconstruct the shape of joint.

Due to this method just requires an image of shadow, the variable reflectivity of joint surface doesn't have any effect in the reconstruction process. Conventional and efficient image process algorithms are good enough to extract the shadow from the PCB. Some consistent characteristics of the shape of solder joint are used to build a shape model to obtain extra constraint conditions which are used to reconstruct the joint totally.

Compare the reconstruction results of this method with that of SFS method, this method can reduce the hardware cost and algorithm complexity significantly, which at the same time obtains better accuracy and efficiency.

2 3-D RECONSTRUCTION OF SOLDER JOINT

There are three steps to reconstruct the solder joint shape. Firstly, a structured light is used to project a shadow of the joint on the PCB and the shadow is captured by a camera. Secondly, the profile of joint and the profile of joint shadow are extracted by image process algorithms. Finally, a shape model and the profiles are used to reconstruct the 3-D surface of the solder joint.

2.1 Shadow Image Acquisition

The first step is to obtain the shadow image. A paralleled light illuminates the joint at a fixed angle and casts a shadow on PCB. In this paper, we used 60° angle and a highlight LED which provided white-light source to illuminate the joint.

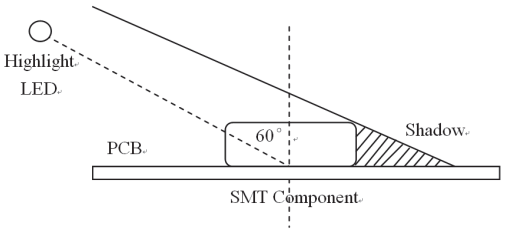

Fig.1 The structured light schematic plot

After locate each SMT component, the image of each individual component can be segmented, the original image is shown in Fig.2.

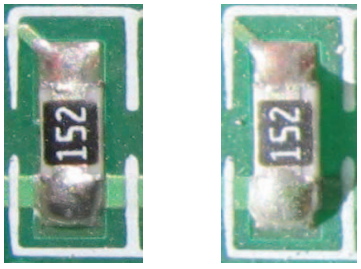

(a) (b)

Fig.2 (a) Original image of SMT component and (b) Original image of component with shadow

2.2 Profile Extraction

Two profiles have to be extracted from the original image. One is the profile of the joint area. The other is the profile of the joint shadow.

Due to the image is gained by color camera and the color of the joint area is distinctive from the PCB background, conventional and slight computation burden image process algorithms are good enough to extract the area of the joint. The distance between color vector $\mathbf{z}$ of the background and color vector $\mathbf{a_0}$ of each pixel can be measured by Eq. (1). $\mathbf{a}$ is the uniformization result of $\mathbf{a_0}$. And if the inequation $D(z,a) \le D_0$ is satisfied, we can confirm which pixel is belonged to the PCB. D_0 is the threshold value of color distance.

$$D(\mathbf{z},\mathbf{a}) = \|\mathbf{z}-\mathbf{a}\| = \left[(z-a)^T (z-a)\right]^{\frac{1}{2}}$$

$$= \left[(z_R-a_R)^2 + (z_G-a_G)^2 + (z_B-a_B)^2\right]^{\frac{1}{2}} \quad (1)$$

$$\mathbf{a} = \mathbf{a_0} \cdot \frac{z_R + z_G + z_B}{a_{0R} + a_{0G} + a_{0B}}$$

Some white paintings on the PCB around the SMT component which interrupted the segmentation process. However, the painting area was thin and small compared with the area of SMT component, so the dilation operation and blob analysis can be used to segment the two areas. The dilation operation and erosion operation are shown in Eq. (2) and Eq. (3).

$$A \oplus B = \left\{ z \mid \left(\hat{B}\right)_z \bigcap A \neq \phi \right\} \quad (2)$$

$$A \Theta B = \left\{ z \mid \left[\left(\hat{B}\right)_z \bigcap A \right] \subseteq A \right\} \quad (3)$$

The result of color segmentation is shown in Fig.3 (a), the result of dilation operation and blob analysis is shown in Fig.3 (b). The results showed that these methods can segment the solder joint area, which at the same time eliminate noises and interruptions from the white paintings.

(a) (b)

Fig.3 (a) Color segmentation image and (b) Blob analysis image

Because of the noise existed in the edge of the joint area, the joint profile was rough, so an average filter was used to smooth the edge of the component area. The average filter is shown in Eq. (4). r_{0i} is the original position of profile

points, r_i is the filtered profile points, m is the filter width.

$$r_i = \frac{1}{2m+1}\sum_{i-m}^{i+m} r_{0i}, i = m+1, 2, \cdots, n-m \quad (4)$$

The joint shadow was difficult to segment for the difference between the shadow region and outside region was not distinctive and the white paintings in the background will disturb the segment process. Furthermore, the rough surface of PCB produced some light spots around the shadow, so some steps were required to segment the shadow region.

The first step was resetting the gray value of each pixel by using piecewise linear function shown in Eq. (5).

$$s_{(x,y)} = \begin{cases} 0 & s_{(x,y)} \le s_{down} \\ s_{(x,y)} & s_{down} < s_{(x,y)} < s_{up} \\ 1 & s_{(x,y)} \ge s_{up} \end{cases} \quad (5)$$

After resetting the gray value, close and open operation which is shown as Eq. (6) and Eq. (7) were used to filter the light spots in the image. These algorithms can eliminate the noise and have only a little effect on the shadow profile.

$$A \circ B = (A \Theta B) \oplus B \quad (6)$$

$$A \bullet B = (A \oplus B) \Theta B \quad (7)$$

Finally, dilation strategy in horizontal direction and threshold method were used to obtain the profile of the shadow completely. The threshold method is shown in Eq. (8).

$$s_{(x,y)} = \begin{cases} 0 & s_{(x,y)} \le s_h \\ 1 & s_{(x,y)} > s_h \end{cases} \quad (8)$$

The result of each step is shown in Fig.4. The obtained shadow was consistent with the shadow in the original image.

(a) (b) (c) (d)

Fig.4 (a) Original Shadow and (b) Piecewise linear function and (c) Close operation and (d) Threshold method

The Fig.5 (a) shows the extracted joint area profile and the Fig.5 (b) shows the extracted shadow profile. These results illustrate that conventional image algorithms are good enough to extract the profiles accurately and reliably.

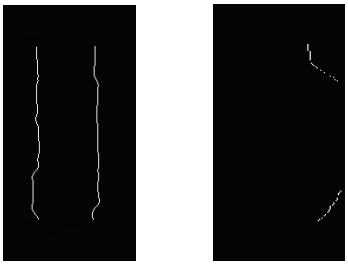

(a) (b)

Fig.5 (a) Extracted Component Profile and (b) Extracted Shadow Profile

2.3 Shape Model Establish and 3-D Reconstruction

A single still shadow which is casted by paralleled light from one direction doesn't provide enough cues to reconstruct the joint completely. However, solder joints present some consistent characteristics in the force of the soldering tin surface tension when the tin is still liquid during the manufactory process, so we can use these characteristics to build a shape model to obtain extra constraint and reconstruct the joint surface completely. The characteristics are summarized as follows:

1) The longitudinal section of the solder joint is similar to a parabola or an arc which is axial symmetry.

2) The longitudinal section which is very close to the component is similar to rectangle and becomes arc or parabola gradually when the distance from the component increase.

3) The height of the solder joint in the edge region is zero.

Some special situations have been excluded, for example: component missing, component location or direction inaccuracy and solder bridged. For these kinds of defects don't follow the characteristics and they can be inspected and excluded by other vision-based algorithms effectively, this method focuses on this specific situation.

From these assumptions, we proposed that in the middle region of the solder joint, the section is a parabola. The parabola figure is shown in Fig.6.

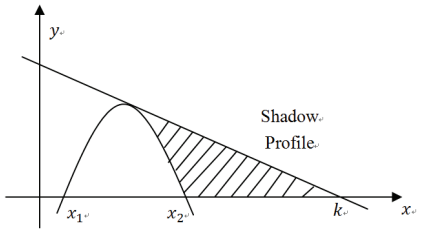

Fig.6 Parabola joint surface and shadow profile

From Fig.6, x_{1i} and x_{2i} are the left and right boundary of each section of solder joint profile, k_i is the boundary of each section of shadow profile. The expression of parabola and the light path are shown in Eq. (9).

$$\begin{cases} y_i = a_i (x - x_{1i})(x - x_{2i}) \\ y_i = -\dfrac{1}{\tan\alpha} x_i + \dfrac{1}{\tan\alpha} k_i \end{cases} \quad i = 1, 2, \cdots, n \quad (9)$$

For the parabola and the light path have only one point of tangency, so Eq. (10) has only one solution.

$$\begin{aligned} & a_i x_i^{\,2} + \left[\frac{1}{\tan\alpha} - a_i \left(x_{1i} + x_{2i} \right) \right] x_i \\ & + \left(a_i x_{1i} x_{2i} - k_i \frac{1}{\tan\alpha} \right) = 0 \end{aligned} \qquad i = 1, 2, \cdots, n \tag{10}$$

In order to make a_i has only one solution in Eq. (10), a_i has to be satisfied with Eq. (11)

$$\begin{aligned} & \left[\frac{1}{\tan\alpha} - a_i \left(x_{1i} + x_{2i} \right) \right]^2 \\ & -4 a_i \left(a_i x_{1i} x_{2i} - k_i \frac{1}{\tan\alpha} \right) = 0 \end{aligned} \qquad i = 1, 2, \cdots, n \tag{11}$$

For a_i should be the smaller one in the two solutions, the solution of a_i is simplified and shown in Eq. (12).

$$a_i = \frac{-B_i - \sqrt{B_i^{\,2} - 4\left(x_{1i} - x_{2i} \right)^2 \frac{1}{\tan^2\alpha}}}{2\left(x_{1i} - x_{2i} \right)^2} \qquad i = 1, 2, \cdots, n$$

$$B_i = 4\frac{1}{\tan\alpha} k_i - 2\frac{1}{\tan\alpha}\left(x_{1i} - x_{2i} \right) \tag{12}$$

The height of each section of the solder joint can be obtained from Eq. (9).

However, the structured light can't project any shadow if a region of the solder joint is flat or not high enough. This region we called Undetectable Region is shown in Fig.7.

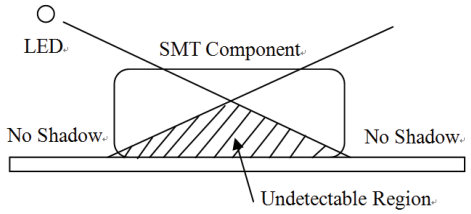

Fig.7 The undetectable region

This situation is very common at the end of the joint. So the shape of the region has to be deduced by other regions which are close to it. We proposed an approach that picking up several control points in the top of each section which is outside the undetectable region and also include the point in the edge of the joint area whose height is zero. Then a cubic spline interpolation was used to deduce the height in the undetectable region. The approach is shown in Fig.8.

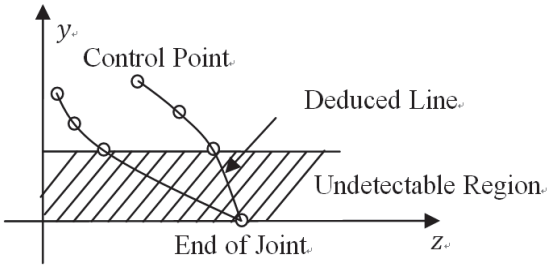

Fig.8 Use control points to deduce the undetectable region

Every section is a cubic function like the Eq. (13) $S_i(z)$, each function has to be satisfied with the Eq. (14).

$$S_i(z) = a_i z^3 + b_i z^2 + c_i z + d_i, i = 0, 1, \cdots, n-1 \tag{13}$$

$$S_i^{(k)}\left(z_i - 0 \right) = S_i^{(k)}\left(z_i + 0 \right), k = 0, 1, 2 \tag{14}$$

For the solder angle is always in the undetectable region, we used cubic spline interpolation to obtain the solder angle, so the cubic spline function is a natural spline. The boundary conditions are shown in Eq. (15).

$$\begin{cases} z_0 = z_{start} \\ z_n = z_{end} \\ S_0''(z_0) = 0 \\ S_n''(z_n) = 0 \end{cases} \tag{15}$$

When the interpolation obtained the height of every undetectable region, the parabola of each region has to be modified and be satisfied with the Eq. (16).

$$a(x - x_{1i})(x - x_{2i}) = S(z_i)\big|_{x = \frac{x_{1i} + x_{2i}}{2}} \tag{16}$$

So the parameter a was calculated and the result is shown in Eq. (17).

$$a = -\frac{4S(z_i)}{\left(x_{1i} + x_{2i} \right)^2} \tag{17}$$

Fig.9 shows the original height and the spline interpolation height. The plot shows that the method can deduce the undetectable region well.

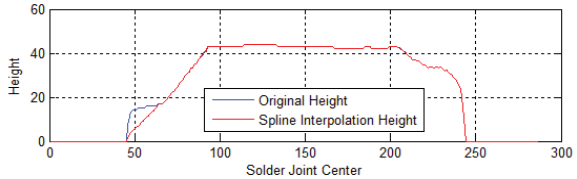

Fig.9 Spline interpolation height plot

From the third characteristic, the section which is very close to the component is rectangle and become arc gradually when the section is further from the component. So a compensation function was proposed to let the reconstruction surface follow this characteristic. The expression of this function is shown in Eq. (18).

$$y_c = e^{-\varphi(z-z_0)} \cdot \left[-a(x-x_{1i})(x-x_{2i}) - \frac{a(x_{1i}-x_{2i})^2}{4} \right]$$

$$z \geq z_0 \qquad (18)$$

z_0 is the position that at the end of the component or at the beginning of the solder joint. We used this function to let the section which is close to the component be rectangle and the effect of the compensation function would be eliminated and decreased when z increases. So the section would change from rectangle to parabola gradually.

The compensate range would be less than $r_{\min}$ at the end of the joint. So parameter φ has to be satisfied with Eq. (19).

$$e^{-\varphi(z_{end}-z_0)} \leq r_{\min} \qquad (19)$$

The value range of φ can be obtained in Eq. (20).

$$\varphi \geq -\frac{In(r_{\min})}{z_{end}-z_0} \qquad (20)$$

This function can make the reconstruction result follow the true shape of solder joint.

3 EXPERIMENT RESULTS

To illustrate the advantages of this method, both the conventional SFS reconstruction method and this method were used to reconstruct the joint shape and the results are shown in Fig.10.

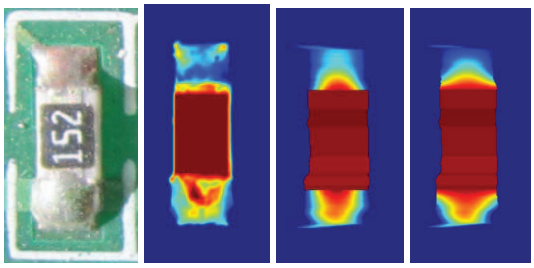

(a) (b) (c) (d)

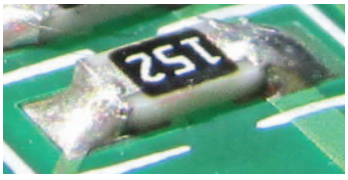

(e)

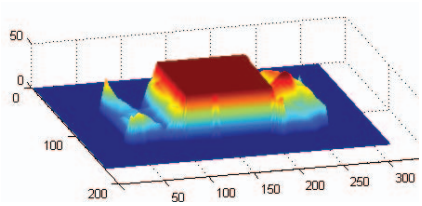

(f)

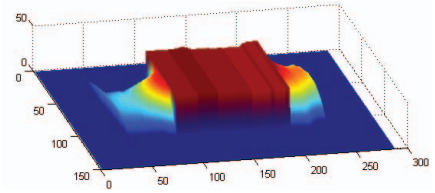

(g)

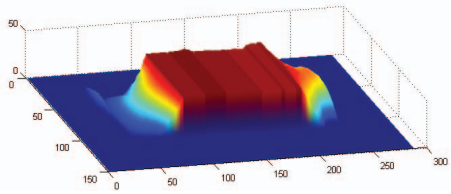

(h)

Fig.10 3-D Reconstruction Result. (a) Original image of SMT component and (b) (f) Conventional SFS reconstruction results and (c) (g) 3-D reconstruction without compensation functions and (d) (h) 3-D reconstruction with compensation functions

The result of SFS reconstruction method is shown in Fig. 10 (b). The reconstructed surface was rough and just a small part of the surface corresponded the true surface, some parts were totally different from the true surface. For example at the end of the joint, the height of joint decreased, however, the reconstruction result showed that the height increased abruptly. This result demonstrated that SFS method is very sensitive to the reflectivity of joint surface and the configuration of structured light. If the assumptions are not met, the reconstruction result would be totally different.

Before using the compensation functions, the result of the method is shown in Fig. 10 (c) (g), the reconstructed surface didn't like the true surface totally in the end of the joint. After added compensation functions, the section region which is close to the component was a rectangle, the shape became parabola gradually and the height of the entire edge region was zero.

Compare the true solder joint shown in Fig. 2 (a) (b) with the reconstructed surface in Fig.10 (d) (h), the reconstructed surface by this method matched the true surface much better than SFS method or the reconstruction result before added compensation functions.

The running time of SFS method and this novel method were measured for 5 times, each running time is shown in Tab.1. Tab. 1 illustrates that this novel method just used less than half time of SFS method to reconstruct.

Table1. Total Running Time

No.	This method	SFS method
1	0.21s	0.62s
2	0.18s	0.36s
3	0.17s	0.36s
4	0.17s	0.37s
5	0.18s	0.36s
Average	0.18s	0.41s

The experiment result illustrated that this novel shadow based 3-D reconstruction method is more accurate than SFS

methods and it is compatible for variable surface conditions. Furthermore, due to the image process and reconstruction algorithms have few complicated calculation, this method is fast and efficient. Only one camera and several highlight LED structured lights were used in the method, so the cost of hardware is lesser than other 3-D reconstruction methods.

Because of the features mentioned above, this method is suitable for large scale application for SMT solder joint 3-D reconstruction with low cost.

4 CONCLUSION

A novel shadow based 3-D reconstruction method for SMT solder joint is proposed in this paper. A paralleled light casts a joint shadow on PCB and then the shadow is captured by a camera and used to reconstruct the joint.

Compared with conventional vision-based SFS method, this 3-D reconstruction method proposed here has advantages such as the following:

1) Due to the shadow won't be affected by the joint surface reflectivity variation, this method is relatively robust, compatible and accurate.

2) Only a single still image is used in the method. The algorithm complexities of shadow extraction and reconstruction are simple so the speed of this method is fast.

3) No special hardware is needed, only a single camera and several highlight LEDs are used in the method. This single camera system avoids the difficult calibration procedure, so the hardware cost is less than other shadow based methods.

In conclusion, this novel method can reconstruct solder joint shape simply, effectively, accurately, efficiently with low hardware cost.

As the method based on a shape model which may not coincide with the real situation totally, more authentic model will be developed to improve the accuracy and determinacy of the reconstruction result in the future research.

Using different color light source for different color PCB may also increase the distinctiveness of shadow and improve the accuracy of shadow extraction.

This method can not only reconstruct SMT solder joints, but also reconstruct other objects which have some consistent characteristics to build a shape model and need to be reconstructed at very high speed with low cost. For example, some simple shape objects like toy components or foodstuff. How to use this method in these fields will be researched in the future.

REFERENCES

[1] Ercal, F., Automatic PCB inspection systems, Potentials, IEEE , vol.14, no.3, pp.6,10, Aug/Sep 1995

[2] Fenglin Guo; Shu-an Guan, Research of the Machine Vision Based PCB Defect Inspection System, Intelligence Science and Information Engineering (ISIE), 2011 International Conference on , vol., no., pp.472,475, 20-21 Aug. 2011

[3] Ziyin Li; Qi Yang, System design for PCB defects detection based on AOI technology, Image and Signal Processing (CISP), 2011 4th International Congress on , vol.4, no., pp.1988,1991, 15-17 Oct. 2011

[4] Madhav Moganti, Fikret Ercal, Cihan H Dagli, et al. Automatic PCB inspection algorithms[J]. Computer Vision and Image Understanding, 1996.

[5] Wang S. J, Zhang Y., Zhang K. Q., etc. 3D Scene reconstruction using panoramic laser scanning and monocular vision[C]. In Proceedings of the 8th World Congress on Intelligent Control and Automation. Jinan, China, 2010, 861-866.

[6] Lopez-Escogido, D.; De Luca, A., 2-D high precision laser sensor for detecting small defects in PCBs, Electrical Engineering, Computing Science and Automatic Control (CCE), 2012 9th International Conference on , vol., no., pp.1,6, 26-28 Sept. 2012

[7] R. Schneider, A. Schick. High-speed optical three-dimensional scanner for automatic solders joint inspection[J]. Society of Photo-Optical Instrumentation Engineers. 1997,36(10):2878~2885

[8] O. Oyeleye, E. A. Lehtihet. Automatic visual inspection of surface mount solder joint defects. International Journal of Production Research. 1999,37(6):1217~1242

[9] E. Guerra, J.R. billalobos. A three-dimensional automated visual inspection system for SMT assembly. Computers & Industrial engineering. 2001,40:175~190

[10] Siewert, T.A;Balzar, D;McCowan, C.N. Nondestructive detection of intermetallics in solder joints by high energy X-ray diffraction Proceedings of 51st Electronic Components and Technology Conference, 2001.

[11] Sumimoto, T;Maruyamay, T;Azuma, Y;Goto, S;Mondo, M;Furukawa, N;Okada, S. Detection of defects at BGA solder joints by using X-ray imagingProceedings of IEEE International Conference on Industrial Technology, 2002.

[12] Martin O;Thomas Z;Wolter K J. X-ray computed tomography onminiaturized solder joints for nano packagingElectronicsPackaging Technology Conference, 2009.

[13] Sheer K. Nayar, Arthur C. shanderson, Lee E. Weiss, David A. Simon, Specular surface inspection using structured highlight and Gaussian images. Robotic and Automation. 1990,6:208~218

[14] Zichao Chen. Automatic optical inspection of surface mounting components Master's thesis [D], National Tsing Hua University in Taiwan. 2004

[15] Shaonong Qiu. Lighting design and feature extraction of solder joint inspection. 2003

[16] Kim T-H;Cho T-H;Moon YS;Park SH. Visual inspection system for the classification of solder joints. Pattern Recognition,1999

[17] Arthur C Sanderson;Lee E. Weiss;Shree K. Nayar. Structured highlight inspection of specular surfaces. IEEE Transactions on Pattern Analysis and Machine Intelligence,1988

[18] B.K.P. Horn, M.J. Brooks(Eds.). Shape from shading. MIT Press. 1989

[19] B.K.P. Horn. Obtaining shape from shading information. In: P.H. Winston(Ed.), The Psychology of Computer Vision, McGraw-Hill. 1975:15~155

[20] Van,Diggelen,J. A photometric investigation of the slopes and heights of the ranges of hills in the maria of the moonBull. Astron. Inst. Netherlands, 1951.

[21] Rindfleisch,T. Photometric method for lunar topography[J]Photogrammetric Engineering, 1966,(2).

[22] J. Oliensis. Uniqueness in shape from shading[J].International Journal of Computer Vision, 1991,(2).

[23] Oliensis J. Shape from shading as a partially well-constrained problem[J].Computer Vision,Graphics,and Image Processing:Image Understanding, 1991,(2).

[24] Michael J. Brooks;Wojciech Chojnacki;Ryszard Kozera. Impossible and ambiguous shading patterns[J].International Journal of Computer Vision, 1992,(2).

[25] Ryszard Kozera. Uniqueness in Shape from Shading Revisited[J].Journal of Mathematical Imaging and Vision, 1997,(2).

[26] B. G. Baumgart, Geometric modeling from computer vision[D]. Standford University, October 1974.

[27] Lorenzi, L.; Melgani, F.; Mercier, G., "A Complete Processing Chain for Shadow Detection and Reconstruction in VHR Images," Geoscience and Remote Sensing, IEEE Transactions on , vol.50, no.9, pp.3440,3452, Sept. 2012

[28] Wohler, C., "3D surface reconstruction by self-consistent fusion of shading and shadow features," Pattern Recognition, 2004. ICPR 2004. Proceedings of the 17th International Conference on , vol.2, no., pp.204,207 Vol.2, 23-26 Aug. 2004

[29] Domrongwatthanayothin, B.; Roeksabutr, A.; Chongchaewchamnanand, M.; Kanjanavapastit, A., "A simple static-shadow based algorithm for 3D complex-terrain surface reconstruction," Geoscience and Remote Sensing Symposium, 2005. IGARSS '05. Proceedings. 2005 IEEE International , vol.3, no., pp.1738,1741, 25-29 July 2005

[30] Iiyama, M.; Koki Hamada; Kakusho, K.; Minoh, M., "Usage of needle maps and shadows to overcome depth edges in depth map reconstruction," Pattern Recognition, 2008. ICPR 2008. 19th International Conference on , vol., no., pp.1,4, 8-11 Dec. 2008

[31] Huihui Song; Bo Huang; Kaihua Zhang, "Shadow Detection and Reconstruction in High-Resolution Satellite Images via Morphological Filtering and Example-Based Learning," Geoscience and Remote Sensing, IEEE Transactions on , vol.52, no.5, pp.2545,2554, May 2014

[32] Rafik Gouiaa, Jean Meunier, 3D reconstruction by fusioning shadow and silhouette information[R]. Canadian Conference on Computer and Robot Vision.

[33] Austin Abrams, Ian Schillebeeckx, Robert Pless, Structure from Shadow Motion[R]. International Conference on Computational Photography, 2014.

[34] Daniel Raviv, Yoh-Han Pao, Kenneth A. Loparo, Reconstruction of Three-Dimensional Surfaces from Two-Dimensional Binary Images[J], IEEE Transactions on Robotics and Automation, 1989.

[35] M. Daum, G. Dudek, On 3-D Surface Reconstruction Using Shape from Shadows[R]. IEEE Conference on Computer Vision and Pattern Recognition, 1998.